

Thermodynamics framework for robust computations of loading-induced anisotropic damage

R. Desmorat, F. Gatuingt & F. Ragueneau

LMT-Cachan, ENS Cachan / Univ. Paris 6 / CNRS

61 av. du président Wilson, F-94235 Cachan Cedex, France

ABSTRACT: Many anisotropic damage models have been proposed for different materials, including concrete. The main drawback of the corresponding analyses is that a large number of material parameters is often introduced, leading to identification difficulties but also to model complexity and associated numerical difficulties. It is also sometimes difficult to ensure the continuity of the stresses if the quasi-unilateral effect of microcracks closure and the dissymmetry tension/compression are represented. We consider here an anisotropic damage model with a restricted number of material parameters (5 including the Young's modulus and Poisson's ratio of the initially isotropic material) and built in the thermodynamics framework. The large dissymmetry of tension/compression response of concrete is due to the loading induced damage anisotropy. A non standard thermodynamics framework is used with damage states represented by a symmetric second order tensor and with a damage rate governed by the positive part of the strain tensor. The proof of the positivity of the intrinsic dissipation is given for any damage law ensuring (anisotropic) damage increase – in terms of positive principal values of the damage rate tensor. This extends then to induced anisotropy the isotropic case property of a positive damage rate. Altogether with the fact that the thermodynamics potential can be continuously differentiated, the considered anisotropic damage model allows for robust Finite Element implementation. Both space and time regularizations are used and applied to quasi-static and dynamic cases. Examples on concrete and reinforced concrete structures are given, with the consideration of either nonlocal Mazars criterion or of Mazars criterion regularized with viscous damage.

1 INTRODUCTION

In standard thermodynamics framework (Halphen and Nguyen, 1975) both the state and the evolution laws derive from potentials, Gibbs free enthalpy $\rho\psi^*$ written in terms of stress $\boldsymbol{\sigma}$ in the present work for the first one, a dissipation or pseudo-dissipation potential for the second one. The elasticity law and the strain energy release rate density \mathbf{Y} , variable associated with \mathbf{D} , are respectively gained as the derivative of the state potential with respect to the elastic strain tensor $\boldsymbol{\epsilon}^e$ and with respect to the damage tensor \mathbf{D} . In the standard framework of thermodynamics a pseudo-dissipation potential quadratic function of \mathbf{Y} is most often considered, the damage law taking the form

$$\dot{\mathbf{D}} = \dot{\lambda} \underline{\mathbf{J}} : \mathbf{Y} \quad (1)$$

with $\dot{\lambda}$ a positive multiplier and $\underline{\mathbf{J}}$ a positive fourth order tensor, eventually nonlinear function of the thermodynamics variables, so that the dissipation $\mathcal{D} =$

$\mathbf{Y} : \dot{\mathbf{D}} = \dot{\lambda} \mathbf{Y} : \underline{\mathbf{J}} : \mathbf{Y}$ due to the degradation mechanisms remains positive for any kind of loading. The choice of damage laws of the form (1) is very restrictive, for instance concerning the possibility to model induced anisotropy directly driven by the strains or the stresses. But, as we will illustrate on numerical examples, to ensure the positivity of the intrinsic dissipation also has good numerical properties.

2 NON STANDARD ANISOTROPIC FRAMEWORK

A general form for the strain energy coupled with anisotropic damage has been proposed by Ladevèze (Ladevèze, 1983; Lemaitre and Desmorat, 2005), as

$$\rho\psi^* = a_1 \text{tr}(\mathbf{H}\boldsymbol{\sigma}\mathbf{H}\boldsymbol{\sigma}) + a_2 \boldsymbol{\sigma} : \boldsymbol{\sigma} + a_3 g(D_H)(\text{tr} \boldsymbol{\sigma})^2 + a_4 (\text{tr} \boldsymbol{\sigma})^2 \quad (2)$$

with $\mathbf{H} = (\mathbf{1} - \mathbf{D})^{-1/2}$ a symmetric tensor and $D_H = \frac{1}{3}\text{tr} \mathbf{D}$, where $g(D_H)$ is a positive increasing function

of D_H , $1/(1 - \eta D_H)$ for example, and where the a_i ($a_1 \geq 0$, $a_3 \geq 0$) as well as $\eta > 0$ are material parameters. The first term of Eq. (2) can take different – non equivalent – forms (Ladevèze, 1983; Papa and Taliercio, 1996; Lemaitre and Desmorat, 2005),

$$a_1 \operatorname{tr} (\mathbf{H}\boldsymbol{\sigma}^D \mathbf{H}\boldsymbol{\sigma}^D) \quad (3)$$

or

$$a_1 \left[\operatorname{tr} (\mathbf{H}\boldsymbol{\sigma}_+ \mathbf{H}\boldsymbol{\sigma}_+) + \langle \boldsymbol{\sigma} \rangle_- : \langle \boldsymbol{\sigma} \rangle_- \right] \quad (4)$$

or

$$a_1 \left[\operatorname{tr} (\mathbf{H}\boldsymbol{\sigma}_+^D \mathbf{H}\boldsymbol{\sigma}_+^D) + \langle \boldsymbol{\sigma}^D \rangle_- : \langle \boldsymbol{\sigma}^D \rangle_- \right] \quad (5)$$

allowing in the last case for the mechanical representation of the quasi-unilateral effect of micro-defects closure, with $\boldsymbol{\sigma}_+$ (resp. $\boldsymbol{\sigma}_+^D$) a special positive part (Ladevèze, 1983; Desmorat, 2000) built from the eigenvalues and the eigenvectors of $\mathbf{H}\boldsymbol{\sigma}$ (resp. of $\mathbf{H}\boldsymbol{\sigma}^D$) and with $\langle \cdot \rangle_-$ the negative part in terms of principal components of a tensor. Two examples of strain energy densities are a first one based on a splitting deviatoric / hydrostatic quantities (with E and ν the Young's modulus and Poisson's ratio of the undamaged material),

$$\rho\psi^* = \frac{1 + \nu}{2E} \operatorname{tr} (\mathbf{H}\boldsymbol{\sigma}^D \mathbf{H}\boldsymbol{\sigma}^D) + \frac{1 - 2\nu}{6E} \frac{(\operatorname{tr} \boldsymbol{\sigma})^2}{1 - \eta D_H} \quad (6)$$

a second one based on the feature of a constant ν/E ratio,

$$\rho\psi^* = \frac{1}{2E} \operatorname{tr} (\mathbf{H}\boldsymbol{\sigma} \mathbf{H}\boldsymbol{\sigma}) + \frac{\nu}{2E} (\boldsymbol{\sigma} : \boldsymbol{\sigma} - (\operatorname{tr} \boldsymbol{\sigma})^2) \quad (7)$$

Concerning the evolution laws, many non standard damage laws can be formulated for induced anisotropy (Mazars et al., 1990; Dragon and Halm, 1996; Lemaitre et al., 2000; Billardon and Pétry, 2005), with second order tensorial damage rate proportional

- to the positive part of the strain tensor $\langle \boldsymbol{\epsilon} \rangle_+$ or to $\langle \boldsymbol{\epsilon} \rangle_+^\alpha$ with α a damage exponent,
- to the absolute value of the plastic strain tensor $\dot{\boldsymbol{\epsilon}}^p$, to the positive part of $\dot{\boldsymbol{\epsilon}}^p$, or to any linear combination $\alpha |\dot{\boldsymbol{\epsilon}}^p| + (1 - \alpha) \langle \dot{\boldsymbol{\epsilon}}^p \rangle_+$,
- to a power $2s$ of the stress tensor,
- to a linear combination $\alpha \langle \boldsymbol{\sigma} \rangle_+^2 + (1 - \alpha) \langle \boldsymbol{\sigma} \rangle_-^2$ (eventually at the power s) where to take $\alpha = 1$ will lead to the modeling of the unilateral damage effect of no damage growth in compression, and to take $1/2 < \alpha < 1$ will lead to the modeling of the quasi-unilateral damage effect of a damage growth in compression smaller than in tension.

Induced damage anisotropy governed by the positive extensions is adapted to quasi-brittle materials as concrete. The other expressions will allow to generalize to induced anisotropy Lemaitre's damage law $\dot{D} = (Y/S)^s \dot{p}$ of a damage rate governed by the accumulated plastic strain rate \dot{p} and enhanced by the strain energy $Y = \frac{1}{2} \boldsymbol{\epsilon}^e : \underline{\mathbf{E}} : \boldsymbol{\epsilon}^e$, with $\underline{\mathbf{E}}$ Hooke's tensor. As possible generalization, one has

$$\dot{D} = \left(\frac{Y}{S} \right)^s \left[\alpha |\dot{\boldsymbol{\epsilon}}^p| + (1 - \alpha) \langle \dot{\boldsymbol{\epsilon}}^p \rangle_+ \right] \quad (8)$$

$$\dot{D} = \left(\frac{\alpha \langle \boldsymbol{\sigma} \rangle_+^2 + (1 - \alpha) \langle \boldsymbol{\sigma} \rangle_-^2}{2ES} \right)^s \dot{p} \quad (9)$$

where E denotes the Young's modulus and S and s the damage parameters. For more details on ductile damage, refer to (Lemaitre and Desmorat, 2005).

The next question will be whether one automatically can ensure the positivity of the dissipation with the simple feature of a positive (tensorial) damage rate \dot{D} .

3 POSITIVITY OF THE INTRINSIC DISSIPATION

Previous elastic energy densities can be continuously differentiated as

$$d\rho\psi^* = \boldsymbol{\epsilon}^e : d\boldsymbol{\sigma} + \mathbf{Y} : d\mathbf{D} \quad (10)$$

or

$$\begin{aligned} d\rho\psi^* = & [2a_1 (\mathbf{H}\boldsymbol{\sigma} \mathbf{H}) + 2a_2 \boldsymbol{\sigma} + 2a_3 g(D_H) \operatorname{tr} \boldsymbol{\sigma} \mathbf{1} \\ & + 2a_4 \operatorname{tr} \boldsymbol{\sigma} \mathbf{1}] : d\boldsymbol{\sigma} + 2a_1 (\boldsymbol{\sigma} \mathbf{H}\boldsymbol{\sigma}) : d\mathbf{H} \\ & + \frac{1}{3} a_3 g'(D_H) (\operatorname{tr} \boldsymbol{\sigma})^2 \operatorname{tr} d\mathbf{D} \end{aligned} \quad (11)$$

leading to a dissipation due to damage mechanisms expressed as

$$\mathcal{D} = \mathbf{Y} : \dot{D} = 2a_1 (\boldsymbol{\sigma} \mathbf{H}\boldsymbol{\sigma}) : \dot{\mathbf{H}} + \frac{1}{3} a_3 g'(D_H) (\operatorname{tr} \boldsymbol{\sigma})^2 \operatorname{tr} \dot{D} \quad (12)$$

For the elastic energy densities written with the terms (3) or (5), the first term $2a_1 (\boldsymbol{\sigma} \mathbf{H}\boldsymbol{\sigma}) : \dot{\mathbf{H}}$ must be replaced by $2a_1 (\boldsymbol{\sigma}^D \mathbf{H}\boldsymbol{\sigma}^D) : \dot{\mathbf{H}}$ or $2a_1 (\boldsymbol{\sigma}_+ \mathbf{H}\boldsymbol{\sigma}_+) : \dot{\mathbf{H}}$ or $2a_1 (\boldsymbol{\sigma}_+^D \mathbf{H}\boldsymbol{\sigma}_+^D) : \dot{\mathbf{H}}$. These terms are next synthetically written $2a_1 (\mathbf{s} \mathbf{H} \mathbf{s}) : \dot{\mathbf{H}}$. With any damage law leading to a positive damage rate tensor, i.e. with positive eigenvalues $(\dot{D})_J$, the term $\operatorname{tr} \dot{D} = \sum_{J=1}^3 (\dot{D})_J$ is positive so that $\frac{1}{3} a_3 g'(D_H) (\operatorname{tr} \boldsymbol{\sigma})^2 \operatorname{tr} \dot{D} \geq 0$. It is important to precise that the eigenvalues $(\dot{D})_J$ of \dot{D}

are not the derivatives \dot{D}_J of the eigenvalues of \mathbf{D} (except in the particular case where \mathbf{D} and $\dot{\mathbf{D}}$ have the same principal directions), the positivity of the eigenvalues $(\dot{\mathbf{D}})_J$ nevertheless implies the increase of the eigenvalues of \mathbf{D} .

Concerning the term $2a_1(\mathbf{sHs}) : \dot{\mathbf{H}}$, note that the expression $\mathbf{H} = (\mathbf{1} - \mathbf{D})^{-1/2}$ rewritten in terms of principal components

$$H_J = \frac{1}{\sqrt{1 - D_J}} \quad (13)$$

gives positive increasing eigenvalues H_J of tensor \mathbf{H} which is then also positive and increasing during any damage process. The positivity of the symmetric matrix (\mathbf{sHs}) is gained by seeking the sign of its eigenvalues, denoted χ , solution of $(\mathbf{sHs})\vec{g} = \chi\vec{g}$, with \vec{g} the corresponding eigenvectors. The eigenvalues χ are equivalently solution of

$$(\mathbf{Hs})^2\vec{g} = \chi\mathbf{H}\vec{g} \quad (14)$$

with obviously $(\mathbf{Hs})^2$ a positive matrix. These eigenvalues take the form

$$\chi = \frac{\vec{g}^T(\mathbf{Hs})^2\vec{g}}{\vec{g}^T\mathbf{H}\vec{g}} \quad (15)$$

and, as ratio of positive terms, are positive. Last, the tensorial product of two symmetric positive tensors (\mathbf{sHs}) and $\dot{\mathbf{H}}$ being positive, one can conclude to the positivity of the intrinsic dissipation \mathcal{D} for any damaging loading, monotonic or not, uniaxial or multiaxial, proportional or non proportional... at the simple condition extended here to anisotropic damage that the damage rate $\dot{\mathbf{D}}$ must remain a positive tensor. Considering conversely the set of states represented by deviatoric tensors $\boldsymbol{\sigma} = \boldsymbol{\sigma}^D$, the dissipation reduced to $2a_1(\mathbf{sHs}) : \dot{\mathbf{H}} \geq 0 \quad \forall (\mathbf{sHs}) \geq \mathbf{0}$ leads to $\dot{\mathbf{H}} \geq \mathbf{0}$, therefore to the fact that $\dot{\mathbf{D}} \geq \mathbf{0}$ is a necessary and sufficient condition for the positivity of the dissipation due to damage $\mathcal{D} = \mathbf{Y} : \dot{\mathbf{D}}$.

4 ANISOTROPIC DAMAGE MODEL FOR CONCRETE

An anisotropic damage model has been proposed for concrete in previous non standard thermodynamics framework (Desmorat, 2004; Desmorat et al., 2007) introducing a single damage variable, a second order tensor, as the representation of the damage state due to microcracking. Mainly due to induced anisotropy, the dissymmetric response of concrete in tension and in compression is obtained with a low number of material parameters: 2 for elasticity, 1 as damage threshold, 2 for damage evolution. Mazars strain damage criterion (Mazars, 1984) is used in this initial model, with the advantage of simplicity for instance at the numerical level.

4.1 Induced anisotropic damage model

For concrete, the microcracks due to tension are mainly orthogonal to the loading direction, when the microcracks due to compression are mainly parallel to the loading direction. The damage state has then to be represented by a tensorial variable \mathbf{D} either a fourth rank tensor or a second rank tensor. The use of a second order damage tensor is more convenient for practical applications (as well as for the material parameters identification) and this is the choice made here. The damage anisotropy induced by either tension or compression is simply modeled by the consideration of damage evolution laws ensuring a damage rate proportional to the positive part of the strain tensor, i.e. a damage governed by the principal extensions (Mazars et al., 1990).

The full set of constitutive equations reads

- Elasticity,

$$\boldsymbol{\epsilon} = \frac{1 + \nu}{E}\tilde{\boldsymbol{\sigma}} - \frac{\nu}{E}tr\tilde{\boldsymbol{\sigma}}\mathbf{1} \quad \text{or} \quad \boldsymbol{\epsilon} = \underline{\mathbf{E}}^{-1} : \tilde{\boldsymbol{\sigma}} \quad (16)$$

- Effective stress,

$$\tilde{\boldsymbol{\sigma}} = [(\mathbf{1} - \mathbf{D})^{-1/2}\boldsymbol{\sigma}^D(\mathbf{1} - \mathbf{D})^{-1/2}]^D + \frac{1}{3}\left[\frac{\langle tr\boldsymbol{\sigma} \rangle_+}{1 - tr\mathbf{D}} + \langle tr\boldsymbol{\sigma} \rangle_-\right]\mathbf{1} \quad (17)$$

- Damage criterion $f = \hat{\epsilon} - \kappa(tr\mathbf{D})$, so that the condition $f < 0 \rightarrow$ elastic loading or unloading, $f = 0, \dot{f} = 0 \rightarrow$ damage growth, where $\hat{\epsilon} = \sqrt{\langle \boldsymbol{\epsilon} \rangle_+ : \langle \boldsymbol{\epsilon} \rangle_+}$ is Mazars equivalent strain and where

$$\kappa^{-1}(\hat{\epsilon}) = aA \left[\arctan\left(\frac{\hat{\epsilon}}{a}\right) - \arctan\left(\frac{\kappa_0}{a}\right) \right] \quad (18)$$

introducing κ_0 as damage threshold, A and a as damage parameters.

- Induced damage anisotropy governed by the positive extensions,

$$\dot{\mathbf{D}} = \dot{\lambda}\langle \boldsymbol{\epsilon} \rangle_+^2 \quad (19)$$

The damage multiplier $\dot{\lambda}$ is determined from the consistency condition $f = 0, \dot{f} = 0$.

The use of a damage criterion function f written in terms of strains instead of stresses allows for a simple implementation in a Finite Element computer code (Desmorat et al., 2007). Even if Euler backward

scheme is used, there is no need of an iterative process. Note that at the final stage of numerical implementation the elasticity law needs to be inverted. This can be done in a closed form as:

$$\begin{aligned} \boldsymbol{\sigma} = & (\mathbf{1} - \mathbf{D})^{1/2} \tilde{\boldsymbol{\sigma}} (\mathbf{1} - \mathbf{D})^{1/2} - \frac{(\mathbf{1} - \mathbf{D}) : \tilde{\boldsymbol{\sigma}}}{3 - \text{tr } \mathbf{D}} (\mathbf{1} - \mathbf{D}) \\ & + \frac{1}{3} [(1 - \text{tr } \mathbf{D}) \langle \text{tr } \tilde{\boldsymbol{\sigma}} \rangle_+ + \langle \text{tr } \tilde{\boldsymbol{\sigma}} \rangle_-] \mathbf{1} \end{aligned} \quad (20)$$

4.2 Extension to nonlocal

Classical mesh dependency occurs when using previous local damage model in a Finite Element code. A nonlocal regularization can be used to gain the mesh independency. One just has to replace local Mazars strain $\hat{\epsilon}$ in the damage criterion f by nonlocal Mazars strain $\hat{\epsilon}^{nl}$ and to consider as nonlocal criterion,

$$f = \hat{\epsilon}^{nl} - \kappa \quad (21)$$

where nonlocal equivalent strain can be defined using an integral form with \mathcal{W} a nonlocal weight function (Pijaudier-Cabot and Bazant, 1987),

$$\hat{\epsilon}^{nl} = \hat{\epsilon}^{nl}(\mathbf{x}) = \frac{1}{V_r} \int_{\Omega} \mathcal{W}(\mathbf{x} - \mathbf{s}) \hat{\epsilon}(\mathbf{s}) ds \quad (22)$$

$$V_r = V_r(\mathbf{x}) = \int_{\Omega} \mathcal{W}(\mathbf{x} - \mathbf{s}) ds$$

or using a second gradient form (Aifantis, 1987; Peerlings et al., 1996),

$$\hat{\epsilon}^{nl} - c \nabla^2 \hat{\epsilon}^{nl} = \hat{\epsilon} \quad (23)$$

Both the integral form (through \mathcal{W}) and the gradient form (through c) introduce a characteristic length l_c . Even if induced anisotropy is considered next, the introduction of a single (isotropic) internal length will prove sufficient for practical applications.

5 VISCOUS REGULARIZATION FOR IMPACT

A regularization possibility for fast dynamics and impact consists in taking into account the strain rate effect on the dynamic response of concrete. For instance, introduce a characteristic time which, altogether with the consideration of the laws of dynamics, will indirectly defines a characteristic length. In the present case of elasticity coupled with damage this can simply be done by introducing a viscosity law $\epsilon_v = \epsilon_v(\dot{D})$ in Mazars criterion. The damage evolution occurs not anymore at $f = 0$ but at $f = \epsilon_v > 0$. A classical law for isotropic damage is Norton-Perzyna power law, $\epsilon_v = k \dot{D}^{1/n}$, with k and n the viscosity parameters. It leads to an unbounded damage rate often too high at high strain rates.

It is possible to bound the damage rate, for instance by the maximum rate $\dot{D}_{\infty} = 1/\tau_c$ material dependent equal to the inverse of the characteristic time τ_c (Allix and Deü, 1997; Ladevèze et al., 1998). To gain this property, these authors rewrite the criterion surface as $f = g(\hat{\epsilon}) - D$ (with $g = \kappa^{-1}$) and define the viscosity law as

$$f = D_v > 0 \quad D_v = -\frac{1}{b} \ln \left(\frac{\dot{D}_{\infty} - \dot{D}}{\dot{D}_{\infty}} \right) \quad (24)$$

from which derives the delay-damage law, saturating at high strain rates,

$$\dot{D} = \dot{D}_{\infty} [1 - \exp(-b(g(\hat{\epsilon}) - D))] \quad (25)$$

The viscosity parameters, material dependent, are then \dot{D}_{∞} and b . This regularization is defined locally (i.e. at a structure Gauss point) and is well adapted for dynamics computations. It can be extended to the case of induced anisotropic damage by setting (Desmorat and Gatuingt, 2006):

$$\text{tr } \dot{\mathbf{D}} = \dot{D}_{\infty} [1 - \exp(-b(\kappa^{-1}(\hat{\epsilon}) - \text{tr } \mathbf{D}))] \quad (26)$$

The full set of constitutive equations now reads

- Elasticity,

$$\boldsymbol{\epsilon} = \frac{1 + \nu}{E} \tilde{\boldsymbol{\sigma}} - \frac{\nu}{E} \text{tr } \tilde{\boldsymbol{\sigma}} \mathbf{1} \quad \text{or} \quad \boldsymbol{\epsilon} = \underline{\mathbf{E}}^{-1} : \tilde{\boldsymbol{\sigma}} \quad (27)$$

- Effective stress,

$$\begin{aligned} \tilde{\boldsymbol{\sigma}} = & [(\mathbf{1} - \mathbf{D})^{-1/2} \boldsymbol{\sigma}^D (\mathbf{1} - \mathbf{D})^{-1/2}]^D \\ & + \frac{1}{3} \left[\frac{\langle \text{tr } \boldsymbol{\sigma} \rangle_+}{1 - \text{tr } \mathbf{D}} + \langle \text{tr } \boldsymbol{\sigma} \rangle_- \right] \mathbf{1} \end{aligned} \quad (28)$$

- Damage criterion (local) $f = \kappa^{-1}(\hat{\epsilon}) - \text{tr } \mathbf{D}$, using the viscous regularization (24),

$$f \leq 0 \longrightarrow \text{elastic loading or unloading}$$

$$f > 0 \quad \text{with} \quad f = -\frac{1}{b} \ln \left(\frac{\dot{D}_{\infty} - \text{tr } \dot{\mathbf{D}}}{\dot{D}_{\infty}} \right) \quad (29)$$

\longrightarrow damage growth

with \dot{D}_{∞} and b the delay-damage parameters.

- Induced damage anisotropy governed by the positive extensions,

$$\dot{\mathbf{D}} = \dot{\lambda} \langle \boldsymbol{\epsilon} \rangle_+^2 \quad (30)$$

The damage multiplier $\dot{\lambda}$ is determined from the damage criterion expression for $f > 0$ (Eq. 29).

The delay-damage law (25) is recovered from previous equations.

Again, the numerical implementation in a Finite Elements computer code is quite simple as – once again – it does not need an iterative process (Desmorat and Gatuingt, 2006).

6 STRUCTURAL EXAMPLES

The local and nonlocal integral anisotropic damage model has been implemented in CEA CAST3M Finite Element code. The anisotropic delay-damage model has been implemented in the explicit code LS-Dyna. The numerical scheme for the time integration is for both cases Euler's backward scheme but solved explicitly (Desmorat and Gatuingt, 2006; Desmorat et al., 2007). Finite Element examples on 3D structures are given next to illustrate the model capabilities.

6.1 Plain concrete mixed-mode fracture

The double edge notched specimen tested by Nooru-Mohamed (Nooru-Mohamed, 1992) is analysed using the implementation of the model developed in the previous section. The specimen is a symmetric 200 mm × 200 mm mortar square with two horizontal notches, 30 mm long and 5 mm thick.

The rotation of the external boundary of the plate is restricted around the vertical axis. The concrete specimen is first loaded by an increasing shear (lateral) force $F(t)$ applied on the lateral surface. During the application of the shear force, the vertical displacement of the upper surface is totally free. In a second time, a vertical displacement $U(t)$ is applied up to failure at constant $F = F_{Max}$, the higher F_{Max} the more curved the crack path.

The case study is here carried out for a lateral load $F_{Max} = 10$ kN. The FE discretization of the specimen is made by the use of four node tetrahedron elements with one integration point. In order to perform the computations in 3D at reasonable cost, a FE mesh with a 5 mm width is used when the real width of the specimen is 50 mm. The model parameters used for the simulation are: $E = 42000$ MPa, $\nu = 0.2$, $\kappa_0 = 5 \cdot 10^{-5}$, $A = 5 \cdot 10^3$, $a = 2.93 \cdot 10^{-4}$. The nonlocal length used in the integral weight function is $l_c = 2$ mm, small value indeed justified by the fact that the material is a mortar with very small constituents (Bazant and Pijaudier-Cabot, 1989; Rague-neau et al., 2003). Three meshes are used: a coarse mesh with a total of 4936 elements, a medium mesh with 11294 elements, and a fine mesh with 14766 elements. The characteristic length corresponds then close to the notch to 2 elements of the coarse mesh, to 8 elements of the medium mesh, to 14 elements of the fine mesh.

Figure 1 shows the anisotropic damage patterns

computed for the different meshes (at the figure top is the cracking pattern experimentally observed (Nooru-Mohamed, 1992)). The left column corresponds to the D_{22} damage field, the right one to the D_{11} damage field, both in nonlocal computations. They exhibit the now classical convergence and mesh independence of the results obtained with a nonlocal model, here in case of anisotropic damage. The application of the shear load up to F_{Max} yields localized damage at the notch tip. The structural failure is then due to the application of the vertical displacement $U(t)$ with mainly mode I cracks represented here in the Continuum Damage Mechanics framework by large D_{22} values. The damage patterns computed corresponds to the crack patterns observed with the rotation of two main cracks represented. The cracks are not perfectly symmetric with respect to the center of the specimen due to the application of the experimental boundary conditions.

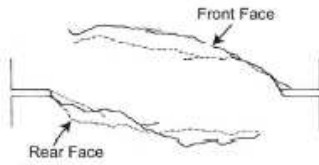
6.2 Reinforced concrete structure

The objectives of this section are to evaluate the robustness and the ability of the anisotropic damage model to deal with a reinforced concrete element subject to flexion. The structure is a reinforced square cross section beam, subject to three point bend loading. Figure 2 shows geometric features for concrete and steel. During loading, multiple loading paths are encountered in different parts of the beam: tension on the lower part, compression on the upper part, shear near the edge and along the reinforcing bars. The corresponding different features of the constitutive equations are activated at the same time and the occurrence during loading of several competitive cracks usually makes difficult the global convergence scheme. For these reasons, this case-study was part of the international MECA benchmark, launched by E.D.F. to compare and discriminate different 3D constitutive models for concrete (Delaplace and Ghavamian, 2003).

For concrete, the material parameters used in the following computations are those of previous section. For steel, elasto-plasticity with linear hardening is considered and the material parameters are imposed by the benchmark: Young's modulus $E = 200000$ MPa, Poisson ratio $\nu = 0.3$, yield stress of 480 MPa, plastic modulus of 20000 MPa. For the computation, a 3D specimen has been meshed with 2 elements in the thickness for a total of 600 eight node parallelepipedic elements. Accounting for the different symmetries of the problem, only one reinforcing steel bar is modelled. The mean dimension of the finite element size is 50 mm.

The monotonic loading is applied up to failure. Two computations with two different characteristic lengths are performed in order to appreciate the effect of the nonlocal length (Gaussian weight function, $l_c = 150$

Experimental cracking path :



for the characteristic length $l_c = 150$ mm.

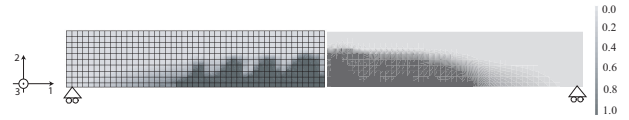


Figure 3: Mesh and D_{11} damage field obtained at the beginning of steels yielding (left : $l_c = 150$ mm, right: $l_c = 250$ mm - left and right correspond to two different computations)

6.3 3D dynamics tension test

In order to get tensile results at very high strain rates, tensile tests by scabbing were developed (Klepaczko and Brara, 2001; Schuler et al., 2006). Figure 4 shows the principle of the test. The setup consists of a striker (launched at the velocity V), an input bar and the tested specimen. The input bar of (Klepaczko and Brara, 2001) experiment has a diameter of 40 mm for a one meter length, while the concrete sample has the same diameter for a length of 120 mm. After the impact of the striker, an incident wave propagates in the input bar. One part of the wave is transmitted into the specimen and another one is reflected at the bar/specimen interface. The transmitted compression wave is reflected at the free end and becomes a tensile wave. This leads to fracture in the spall plane.

Three Finite Element meshes have been used. A coarse mesh is made of 24000 underintegrated 8-nodes brick elements, a medium mesh of 48000 elements and a fine mesh of 96000 elements. At time $t = 0$ the mesh boundaries are free and the experimental pressure wave is applied on the right face of the specimen. The simulation of the test must make it possible to find the rupture of the sample experimentally observed, *i.e.* a single main rupture crack at the distance $X = 65.8$ mm of the impacted face.

Figure 5 shows the damage field D_{11} associated with the axial axe \vec{e}_1 . When the material is subjected to compression the imposed strain is not sufficient to damage the material. To the opposite, when the state of tension becomes sufficiently large after the compressive wave reflection on the free surface, one obtains a damage D_{11} close to 1 in a cross section. This cross section, which represents the location in which cracking will be initiated, is located at a distance X ranging between 64 and 69 mm from the impacted face. This measure is in good agreement with experimental one.

In order to illustrate the mesh independency (due

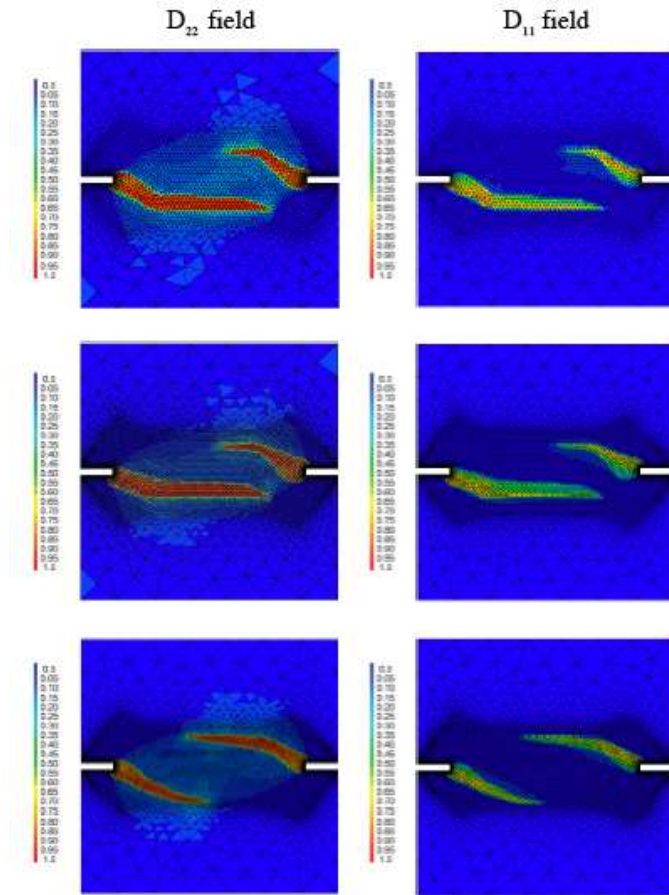


Figure 1: Damage maps for Nooru-Mohamed test at $U = 3.5 \cdot 10^{-3}$ mm/s (a) left column: D_{22} fields, (b) right column: D_{11} fields

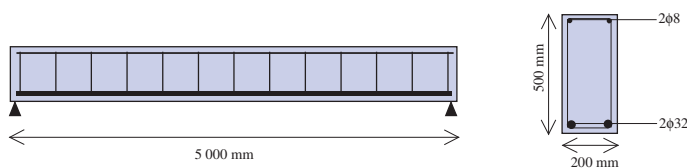


Figure 2: Reinforced concrete beam

mm and $l_c = 250$ mm). The choice $l_c = 150$ mm is the more physical as it corresponds here to a characteristic length equal to 3 or 4 times the maximum aggregate size (Bazant and Pijaudier-Cabot, 1989).

As one can see in the D_{11} -damage maps given in Figure 3, due to the reinforcing steel bar implying a flexural rupture the effect of the characteristic length is important on the cracking pattern as it can be seen from damage maps. The choice $l_c = 150$ mm is the more appropriate here, as expected. The computation represents quite well the multiple cracks propagation

Figure 4: Principle of the dynamic tension test

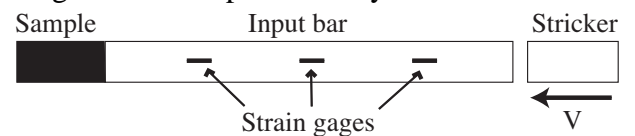
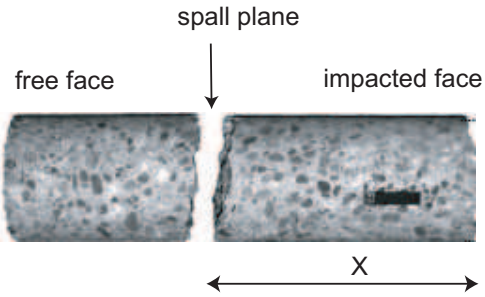
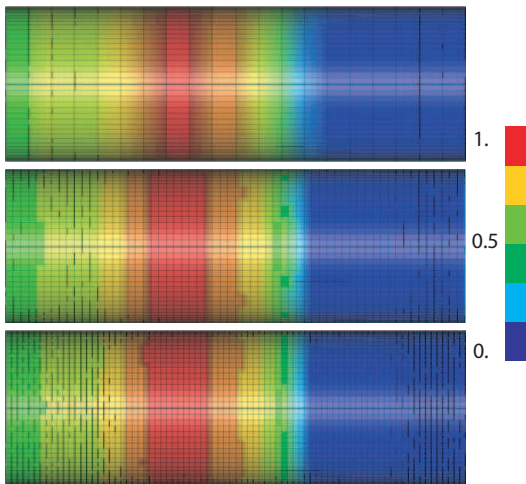


Figure 5: Damage in the concrete sample
Experimental



Numerical



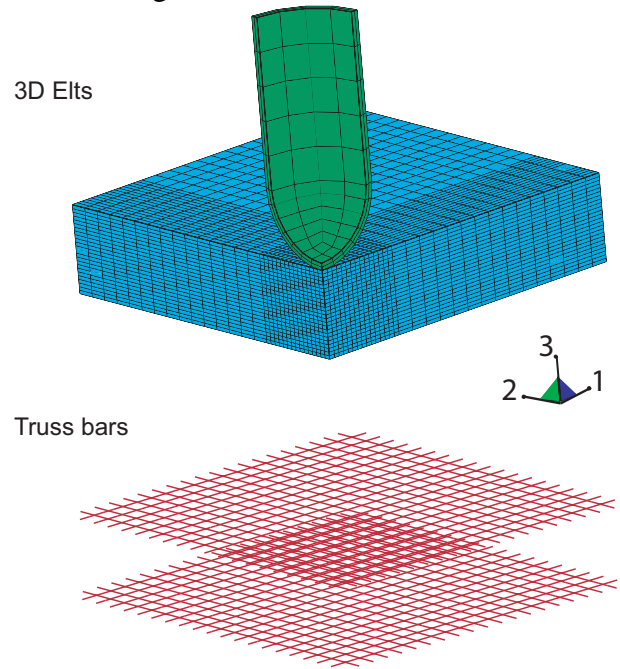
to the viscous regularization of the delay-damage model), the results are presented on the coarse, medium and fine meshes. The damage maps obtained for the three meshes are shown in Figure 5. One can notice that the width of the localized damage band is the same for the three meshes and equal to approximately $5 \times l_c$, therefore of the order of magnitude of a characteristic length introduced from the knowledge of the wave celerity c_L , $l_c = c_L \times \tau_c = c_L / D_\infty$. Note that the time steps are different in the three simulations due to the Courant's condition based on the mesh size.

6.4 Impact on a reinforced concrete slab

In order to evaluate the ability of the anisotropic damage model to describe the concrete behavior in a case rather complex but representative of an industrial application, a test in which a projectile impacts a concrete slab has been carried out. The projectile is a cylinder representative of a Cessna engine (masse=200 kg, velocity=83,3 m/s, cross section= 1 m^2) with an elastic behavior.

Figure 6 shows the finite element mesh used for the simulations on a 4 meters width and 0.5 meters thick slab. The slab is meshed with 24000 3D under-integrated elements and the reinforcements are repre-

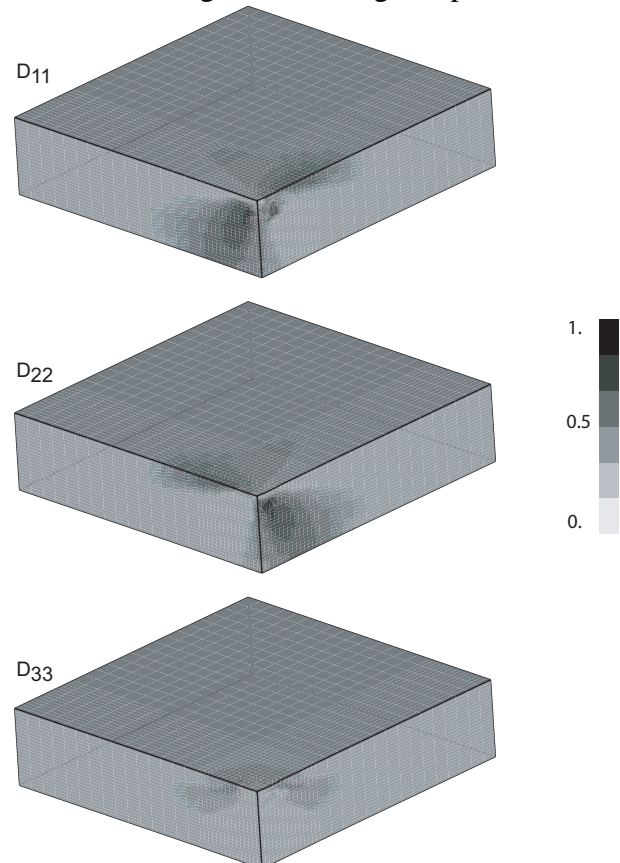
Figure 6: Finite Element mesh



sented by 2300 truss-bars. The impacted area has a refined mesh whereas the other part of the slab has a coarse one.

Figure 7 shows the damages D_{11} , D_{22} and D_{33} into the slab. One can notice that due to the symmetry condition, the damage D_{11} and D_{22} have a similar pattern. The damage D_{33} represents the cracks in the slab thickness and is representative of the scabbing phe-

Figure 7: Damage map



nomenon. In our simulation, damages D_{11} and D_{22} are quite large exhibiting a shear rupture of the concrete slab with the apparition of a punch cone as experimentally observed in cases of thin slabs. In the same time, the damage D_{33} remains small and does not exhibit scabbing.

7 CONCLUSION

A non standard thermodynamics framework for induced anisotropic damage guaranties the positivity of the intrinsic dissipation. A proof is given and the scalar feature $\dot{D} \geq 0$ of a positive damage rate for isotropic modeling is extended to anisotropy as the simple feature $\dot{\mathbf{D}} \geq 0$ of a positive damage rate tensor. The convexity of the state potential with respect to the damage variable is not necessary.

An anisotropic damage model is described in the previous non standard framework, with a quite low numbers of material parameters (5 including the elasticity parameters for the initial plus an internal length for the nonlocal model or plus 2 viscosity parameters for the delay-damage model). The good mathematical properties of the model (differentiability of the state potential, positivity of the dissipation due to anisotropic damage even for complex non proportional loading) prove to be efficient for numerical computations of 3D structures, in both quasi-static and dynamic cases.

REFERENCES

- Aifantis, E. (1987). The physics of plastic deformation. *Int. J. Plasticity*, 3:211–247.
- Allix, O. and Deü, J. (1997). Delay-damage modelling for fracture prediction of laminated composites under dynamic loading. *Engineering Transactions*, 45:29–46.
- Bazant, Z. P. and Pijaudier-Cabot, G. (1989). Measurement of characteristic length of nonlocal continuum. *Journal of Engineering Mechanics*, 115:755–767.
- Billardon, R. and Pétry, C. (2005). Creep damage behaviour of a copper alloy on a large temperature range. In *ASME/ASCE/SES Conference on Mechanics and Materials (McMat2005)*, 1-3 juin, Baton Rouge, Louisiana, USA.
- Delaplace, A. and Ghavamian, S. (2003). *Modèles de fissuration de béton - projet MECA*, volume 7(5). Revue Française de Génie Civil, Lavoisier.
- Desmorat, R. (2000). Quasi-unilateral conditions in anisotropic elasticity. *C.R. Acad. Sci. Paris, série IIB*, 328:445–450.
- Desmorat, R. (2004). Modèle d'endommagement anisotrope avec forte dissymétrie traction/compression. In *5è journées du Regroupement Francophone pour la Recherche et la Formation sur le Béton (RF2B)*, Liège, Belgium, 5-6 july.
- Desmorat, R. and Gatuingt, F. (2006). Anisotropic 3d delay-damage model for concrete. *Int. J. Materials and Product Technology*, in press.
- Desmorat, R., Gatuingt, F., and Ragueneau, F. (2007). Nonlocal anisotropic damage model and related computational aspects for quasi-brittle materials. *Engineering Fracture Mechanics*, in press.
- Dragon, A. and Halm, D. (1996). Modélisation de l'endommagement par mésosfissuration : comportement unilatéral et anisotropie induite. *C. R. Acad. Sci., Série IIB*, 322:275–282.
- Halphen, B. and Nguyen, Q. (1975). Sur les matériaux standards généralisés. *J. de Mécanique*, 14:39–63.
- Klepaczko, J. and Brara, A. (2001). An experimental method for dynamic tensile testing of concrete by spalling. *Int. Journal of Impact Engineering*, 25:387–409.
- Ladevèze, P., Allix, O., Gornet, L., Leveque, D., and Perret, L. (1998). *TComputational damage mechanics approach for laminates: identification and comparison with experimental results*, chapter Damage Mechanics in Engineering Materials. Section A. Elsevier, G. Voyiadjis ed.
- Ladevèze, P. (1983). On an anisotropic damage theory. In *Proc. CNRS Int. Coll. 351 Villars-de-Lans, Failure criteria of structured media*, J. P. Boehler ed. 1993, pages 355–363.
- Lemaitre, J. and Desmorat, R. (2005). *Engineering Damage Mechanics : Ductile, Creep, Fatigue and Brittle Failures*. Springer.
- Lemaitre, J., Desmorat, R., and Sauzay, M. (2000). Anisotropic damage law of evolution. *Eur. J. Mech., A/ Solids*, 19:187–208.
- Mazars, J. (1984). *Application de la mécanique de l'endommagement au comportement non linéaire et à la rupture du béton de structure*. PhD thesis, Thèse d'Etat Université Paris 6.
- Mazars, J., Berthaud, Y., and Ramtani, S. (1990). The unilateral behavior of damage concrete. *Eng. Fract. Mech.*, 35:629–635.
- Nooru-Mohamed, M. (1992). *Mixed-mode fracture of concrete: An experimental approach*. PhD thesis, Delft University of Technology, The Netherlands.
- Papa, E. and Taliercio, A. (1996). Anisotropic damage model for the multi-axial static and fatigue behaviour of plain concrete. *Engineering Fracture Mechanics*, 55:163–179.
- Peerlings, R., de Borst, R., Brekelmans, W., and de Vree, J. (1996). Gradient-enhanced damage model for quasi-brittle materials. *Int. J. Num. Meth. Engng*, 39:391–403.
- Pijaudier-Cabot, G. and Bazant, Z. (1987). Nonlocal damage theory. *J. Engng Mech., ASCE*, 113:1512–1533.
- Ragueneau, F., Delaplace, A., and Davenne, L. (2003). Mechanical behavior related to continuum damage mechanics for concrete. *Revue Française de Génie Civil*, 7:635–645.
- Schuler, H., Mayrhofer, C., and Thoma, K. (2006). Spall experiments for the measurement of the tensile strength and fracture energy of concrete at high strain rates. *International Journal of Impact Engineering*, 32:1635–1650.